

Finite-Temperature Quantum-Rotor Approach for Ultracold Bosons in Optical Lattices

M. Rodríguez Martín and T. A. Zaleski

Institute of Low Temperature and Structure Research, PAS, Okólna 2, 50-422 Wrocław, Poland

Interacting bosons in optical lattices directly expose quantum phases in a clean, highly controllable environment. This requires engineering systems with very low entropies, but the resulting temperature–interaction ratios T/U of present experiments remain well above the domain where zero-temperature theories are expected to be reliable. The quantum-rotor approach (QRA), while analytically powerful and extremely flexible, inherits ground-state phase correlations and therefore breaks down once thermal winding of the phase field becomes significant. Here we construct a finite-temperature extension of QRA by (i) performing resummation of winding-number contributions for temperatures $k_B T/U \lesssim 0.2$ and (ii) developing an auxiliary-variable expansion that remains accurate toward the classical limit. The resulting closed expression for the phase correlator is inserted into the standard spherical-approximation QRA without sacrificing the method’s flexibility with respect to lattice geometry and dimensionality. The approach reproduces the shrinkage of Mott lobes from $T = 0$ up to $k_B T/U \simeq 0.2$ in quantitative agreement with theoretical predictions and with *in-situ* imaging experiments. This *finite-T QRA* thus supplies an analytic, computationally light tool for strongly correlated lattice bosons and sets the stage for amplitude-fluctuation upgrades required at higher temperatures.

I. INTRODUCTION

The past two decades have witnessed the transformation of ultracold-atom systems from delicate few-body curiosities into fully fledged *quantum simulators* of strongly correlated lattice models. When a degenerate gas of bosonic atoms is loaded into an optical standing-wave potential, its low-energy physics is accurately captured by the Bose–Hubbard Hamiltonian [1, 2]. By tuning t/U (tunneling amplitude vs. on-site interaction) one can drive a quantum phase transition between a compressible superfluid (SF) and an incompressible Mott insulator (MI). The earliest observation of this transition through time-of-flight interference fringes already established optical lattices as clean realizations of paradigmatic condensed-matter models [3]. Today, quantum-gas microscopes provide single-site resolution of density and coherence, allowing *in situ* snapshots of individual atoms and defects [4, 5].

In solid-state materials the absolute lattice temperature (in kelvin) is the natural metric because both the coupling constants and the environment are fixed. In an optical lattice, by contrast, the interaction scale U is *engineered* and typically lies in the tens of nanokelvin range; moreover the lattice is raised almost adiabatically. Under near-isentropic loading the entropy per particle, $s = S/N$, is conserved to a good approximation, and the final temperature therefore adjusts until the ratio $k_B T/U$ satisfies this en-

tropy constraint [6]. Reaching low *dimensionless* temperatures, e.g. $k_B T/U \lesssim 0.05$, for bosonic MI order, thus hinges on cooling the *entropy reservoir* rather than the thermometer reading in nanokelvin.

Precise thermometry in optical-lattice experiments remains notoriously hard because the lattice suppresses conventional probes; as McKay and DeMarco stress, reliable T estimates almost always rely on matching *in-situ* or parity-projected density profiles to quantum-Monte-Carlo calculations rather than on direct fitting of time-of-flight images [7]. Even with that caveat, present bosonic systems sit surprisingly “*warm*” on the interaction scale set by U : most laboratories report $k_B T/U \sim 0.1 – 0.25$. Early single-site microscopes already reached $k_B T/U = 0.15$ in the first images of the superfluid–Mott crossover [4]; subsequent Rb work found $k_B T/U = 0.09$ for $n = 1$ (one atom per site) shell and 0.074 for $n = 2$ [5]. Similar values, $k_B T/U \approx 0.1 – 0.21$, were obtained for non-cooled Yb MI samples [8], while very light ^7Li gave $k_B T/U \approx 0.1$ (with a lower bound of 0.083 inferred from fits) [9]. The current record belongs to Yang et al., who combined staggered-immersion cooling with sublattice entropy removal to push a two-dimensional Rb array down to $k_B T/U = 0.046$ and a homogeneous entropy of only $1.9 \times 10^{-3} k_B$ per particle [10]. Although the absolute temperatures lie in the ten- to hundred-nano-kelvin range, they are comparable to U , underscoring the challenge of cooling into the deep-quantum regime where

$k_B T \ll U$. Thus, while genuine low-entropy magnetism still lies ahead, today's benchmarks unanimously place experimental bosons at $k_B T/U \gtrsim 0.05$, with most data clustered around 0.1–0.25.

Capturing correlation physics in this entropy-limited regime is a problematic theoretical challenge. Mean-field and local-density approximations neglect critical phase fluctuations and therefore overestimate T_c , t_c/U and compressibility [11, 12]. Strong-coupling perturbative-DMRG treatments are well-fitted for $k_B T/U \lesssim 0.2$, however require that tunnelling is small [13, 14]. On the other hand, controlled QMC simulations provide the gold standard for equilibrium benchmarks [15–17], yet their computational cost scales significantly with system size and inverse temperature, rendering them impractical for rapid scans across lattice geometries or parameter space. To this end, an analytic, geometry-agnostic approach that remains quantitatively reliable for $k_B T \lesssim U$ could be very useful.

The quantum-rotor approach (QRA) meets part of this need: by integrating out amplitude fluctuations and focusing on phase dynamics, it yields closed-form expressions for the order parameter and phase boundary that automatically incorporate lattice density of states and dimensionality [18]. At zero temperature it reproduces the universal shape of Mott lobes and their critical exponents. Its scope, however, extends far beyond static phase boundaries. The method quantitatively reproduces the time-of-flight (TOF) momentum distributions seen in clean lattices and, crucially, in the presence of synthetic magnetic fields of arbitrary gauge [19–21]. By convolving the QRA phase propagator with a Bogoliubov treatment of density modes, it yields single-particle spectral functions $A(\mathbf{k}, \omega)$ across superfluid and Mott regimes, capturing the persistence (or loss) of sharp coherence peaks and the transfer of spectral weight [22, 23]; or predicts dynamic structure factor $S(\mathbf{k}, \omega)$ directly measurable by Bragg spectroscopy [24]; or allows to compute momentum-resolved longitudinal conductivity, predicting linear low- k behavior [25]. However, its principal weakness remains intrinsic: the phase correlator is still evaluated with *ground-state* statistics, so thermal winding numbers are omitted. Although it still can be used to approximate the low-temperature regime [26, 27], the standard quantum rotor approach may lead to oversharpened SF–MI crossover and underestimation of the compressibility when $k_B T/U \gtrsim 0.0022$.

In the present paper we construct a finite-temperature extension of the quantum rotor model that remains quantitatively accurate up to $k_B T/U \approx 0.2$. Two complementary analytic expansions are developed: (1) winding-number resummation; (2) auxiliary-field (high- T) expansion with small parameter being $1/\beta U$. Both yield closed expressions for the phase correlator that drop into the spherical approximation without increasing computational effort. We show that the resulting phase diagram and density profiles reproduce theoretical predictions and experimental in-situ microscopy observations. The extended rotor framework thus furnishes a versatile, computationally light tool for strongly correlated lattice bosons, while its construction points the way toward incorporating amplitude fluctuations and addressing even higher-temperature, normal-fluid regimes.

II. QUANTUM ROTOR APPROACH TO THE BOSE HUBBARD MODEL

The Bose Hubbard model describes interacting bosons in a periodic lattice with hopping between neighboring sites in the tight-binding scheme [2]. The Hamiltonian hence consists of an onsite interaction term proportional to U , a hopping term dependent on the hopping matrix t_{ij} , and a term proportional to the chemical potential μ , that controls the number of particles:

$$H = \frac{U}{2} \sum_i n_i (n_i - 1) - \sum_{\langle i,j \rangle} t_{ij} a_i^\dagger a_j - \mu \sum_i n_i, \quad (1)$$

where a_i^\dagger , a_i and $n_i = a_i^\dagger a_i$ are the usual bosonic creation, annihilation and number operators, respectively. Throughout this paper we will make use of units in which $U = 1$ and define a shifted chemical potential $\bar{\mu} = \mu + 1/2$.

Here, we employ the Quantum Rotor Approach (QRA) to study the Bose Hubbard model [18]. In the QRA, we make use of a path integral formulation with a Wick rotation of the inverse temperature, $\beta = 1/k_B T$, into imaginary time, τ , writing the partition function as

$$Z = \int \mathcal{D}\bar{a} \mathcal{D}a e^{-S[\bar{a}, a]}, \quad (2)$$

with the action defined by

$$S[\bar{a}, a] = \sum_i \int_0^\beta d\tau [\bar{a}_i(\tau) \partial_\tau a_i(\tau) + H(\tau)]. \quad (3)$$

After getting rid of the quartic term with Hubbard-Stratonovich transformation by means of an auxiliary field $V_i(\tau) = V_i + \partial_\tau \phi_i(\tau)$, a local gauge transformation $a_i(\tau) \mapsto b_i(\tau) e^{i\phi_i(\tau)}$ introduces bosonic fields (amplitude and phase) in terms of which the problem is reformulated underscoring the importance of the phase coherence in formation of the superfluid state. It is important to note that the phase fields $\phi_i(\tau)$ must be periodic modulo 2π in imaginary time, $\phi_i(\tau + \beta) - \phi_i(\tau) = 2\pi n_i$, with $n_i \in \mathbb{Z}$ being the winding numbers.

The b_i fields are then integrated out via a saddle point approximation leading to an effective description in terms of the phase fields, which defines a new phase order parameter $\psi = \langle e^{i\phi_i(\tau)} \rangle$. The phase-only action is given by

$$S[\phi] = \sum_i \int_0^\beta d\tau \left(\frac{1}{2} \dot{\phi}_i^2(\tau) + i\bar{\mu}\dot{\phi}_i(\tau) \right) + \sum_{\langle i,j \rangle} t_{ij} |b_0|^2 \int_0^\beta d\tau \cos(\phi_i(\tau) - \phi_j(\tau)) \quad (4)$$

with $\dot{\phi}_i(\tau) = \partial_\tau \phi_i(\tau)$ and $|b_0|^2 = (zt + \bar{\mu})/U$ being the static part of the $b_i(\tau)$ fields, i.e. $b_0 = \langle b_i(\tau) \rangle$, where z is the coordination number and $t = t_{ij}$ (for hopping between the nearest neighbors).

It is now convenient to introduce a unimodular field $z_i(\tau)$ via the resolution of the identity

$$1 = \int \mathcal{D}\bar{z} \mathcal{D}z \prod \delta(z_i(\tau) - e^{i\phi_i(\tau)}) \times \delta(\bar{z}_i(\tau) - e^{-i\phi_i(\tau)}). \quad (5)$$

Next, we make use of the spherical approximation [28, 29], which consists on relaxing the unimodularity of $z_i(\tau)$, $\bar{z}_i(\tau) z_i(\tau) = 1$, to an average unimodularity, $\frac{1}{N} \sum_i \bar{z}_i(\tau) z_i(\tau) = 1$, by means of a Lagrange multiplier λ :

$$\delta \left(\sum_i \bar{z}_i(\tau) z_i(\tau) - N \right) \propto \int_{-i\infty}^{+i\infty} d\lambda \exp \left(N\lambda - \lambda \sum_i \bar{z}_i(\tau) z_i(\tau) \right). \quad (6)$$

After a Fourier transform into momentum and Matsubara frequency space, we are left with a diagonal action:

$$S[\bar{z}, z] = \frac{1}{\beta N} \sum_{\vec{k}, \omega} \bar{z}(\vec{k}, \omega) \left(\lambda - |b_0|^2 T(\vec{k}) + \gamma^{-1}(\omega) \right) z(\vec{k}, \omega), \quad (7)$$

where $T(\vec{k})$ is the dispersion relation for the lattice, and $\gamma(\omega)$ is the Fourier transform of the phase correlator $\langle e^{i\phi_i(\tau) - i\phi_i(\tau')} \rangle$, which will be studied in detail in the next section.

The partition function is obtained after integrating out the $z_i(\tau)$ field reads:

$$Z = \int d\lambda \exp \left(N\beta\lambda + \sum_{\vec{k}, m} \ln G(\vec{k}, \omega_m) \right), \quad (8)$$

where

$$G(\vec{k}, \omega_m) = \left(\lambda - |b_0|^2 T(\vec{k}) + \gamma^{-1}(\omega_m) \right)^{-1} \quad (9)$$

is the propagator, $\omega_m = 2\pi m/\beta$ is the Matsubara frequency and $m \in \mathbb{Z}$. For a large number of lattice sites N , the steepest descent method gives the value of the Lagrange multiplier by fulfilling the following condition:

$$\frac{1}{N\beta} \sum_{\vec{k}, m} G(\vec{k}, \omega_m) = 1. \quad (10)$$

In the superfluid region, the Lagrange multiplier sticks to the value $\lambda_{SF} = |b_0|^2 T(0) - \gamma^{-1}(0)$, which signals the emergence of the ordered phase by the divergence of the susceptibility. One thus obtains the equation for the order parameter

$$1 - \psi^2 = \frac{1}{N\beta} \sum_{\vec{k}, m} G(\vec{k}, \omega_m). \quad (11)$$

It is useful to introduce now the density of states $\rho(x) = \frac{1}{N} \sum_{\vec{k}} \delta(x - T(\vec{k}))$, in terms of which the previous equation is written simply as:

$$1 - \psi^2 = \int dx \rho(x) \frac{1}{\beta} \sum_m \frac{1}{\lambda - |b_0|^2 x + \gamma^{-1}(\omega_m)}. \quad (12)$$

In the present paper, we are only making use of the density of states corresponding to the simple cubic lattice. However, it is straightforward to extend the results to other geometries simply by choosing $\rho(x)$ appropriately [27, 30–32].

III. COMPUTATION OF THE CORRELATOR

The finite temperature effects on the QRA are mainly encoded in the phase correlator, which can be written as a sum over winding numbers:

$$\gamma(\omega_m) = \frac{1}{Z_0} \sum_{n=-\infty}^{\infty} e^{-\beta(n-v(\mu))^2/2} \times \frac{1}{1/4 - (n-v(\mu) - i\omega_m)^2}, \quad (13)$$

with the free rotors partition function $Z_0 = \sum_{n=-\infty}^{\infty} e^{-\beta(n-v(\mu))^2/2}$ and the function $v(x) = x - \lfloor x \rfloor - 1/2$, where $\lfloor x \rfloor$ denotes the floor function, which gives the greatest integer less than or equal to x (the periodicity of $v(x)$ is a direct consequence of the periodicity of the phase variables at each lattice site).

It should be noted that in the equation of state in Eq. (12) the inverse of the correlator is used, which requires it to be in closed and simple form to be able to perform the summation of the Matsubara frequencies. In the original QRA method in Ref. [18] the phase correlator was evaluated in the zero-temperature limit $\beta \rightarrow \infty$, in which the summation in Eq. (13) simplified to just one leading term with the winding number n_{min} , for which the $n - v(\mu)$ was minimal, i.e.:

$$\gamma^{-1}(\omega_m) = 1/4 - (n_{min} - v(\mu) - i\omega_m)^2. \quad (14)$$

For the general form of the correlator, the sum of the series in Eq. (13) does not exist in a closed form. To go beyond the zero-temperature limit, in the following we present two different approximations which allow to obtain closed form of the inverse correlator on the Matsubara frequencies and perform the summation in Eq. (12).

A. Winding number expansion

The simplest approximation, which constitutes a low temperature expansion, is based on taking into account more than one winding number in the Eq. (13). These winding numbers should provide the leading terms of the sum, which again, occurs when the values of $n - v(\mu)$ are the lowest. A compact way of writing this is by defining $\tilde{v}(\mu) = v(\mu) + \lfloor 2\{\mu\} \rfloor (1 - 2\{\mu\})$, which maps the fractional part to the interval $[0, 1/2]$ symmetrically around $1/2$, and making use of the symmetry (antisymmetry) of the real (imaginary) part

of the correlator with respect to this mapping. In the simplest case, we take the two leading winding numbers:

$$\gamma(\omega_m) \approx \frac{1}{Z_0} \left\{ \frac{e^{-\beta\tilde{v}^2(\mu)/2}}{1/4 - (\tilde{v}(\mu) - (-1)^{\lfloor 2\{\mu\} \rfloor} i\omega_m)^2} + \frac{e^{-\beta(\tilde{v}(\mu) + 1)^2/2}}{1/4 - (\tilde{v}(\mu) + 1 - (-1)^{\lfloor 2\{\mu\} \rfloor} i\omega_m)^2} \right\} \quad (15)$$

The higher the temperature, the more winding numbers need to be taken into account in this approximation. However, just two winding numbers appear to provide a very good approximation of the original correlator up to temperatures of the order $\beta \sim 1/U$ ($k_B T \sim U$), where the difference starts to be considerable. This can be checked by comparing the values provided by Eq. (15) with numerical evaluation of Eq. (13) for large range of n (in our case, $n = -300, \dots, 300$). The results are shown in Figure 1. The temperatures shown for the real (Re) and imaginary (Im) parts differ. Each panel in Fig. 1 includes one temperature where the approximation agrees with the numerical result and one where deviations become noticeable, to indicate the range of validity.

It can be noted that the accuracy of the two-winding number expansion could be improved by generalizing the forms of numerators in the Eq. (15) to read:

$$\gamma(\omega_m) = \frac{a(\beta, \mu)}{1/4 - (\tilde{v}(\mu) - (-1)^{\lfloor 2\{\mu\} \rfloor} i\omega_m)^2} + \frac{b(\beta, \mu)}{1/4 - (\tilde{v}(\mu) + 1 - (-1)^{\lfloor 2\{\mu\} \rfloor} i\omega_m)^2} \quad (16)$$

with a and b being interpolating functions and fitting their values so the formula in Eq. (16) reproduces numerically calculated values of the correlator better than the one in Eq. (15). However, this does not seem to significantly broaden the approximation's usable temperature range while simultaneously rendering its justification and controllability more uncertain.

The proposed approximation leads to rational expressions for the inverse correlator, which can be decomposed into partial fractions. As a result, the summation of the propagator over Matsubara

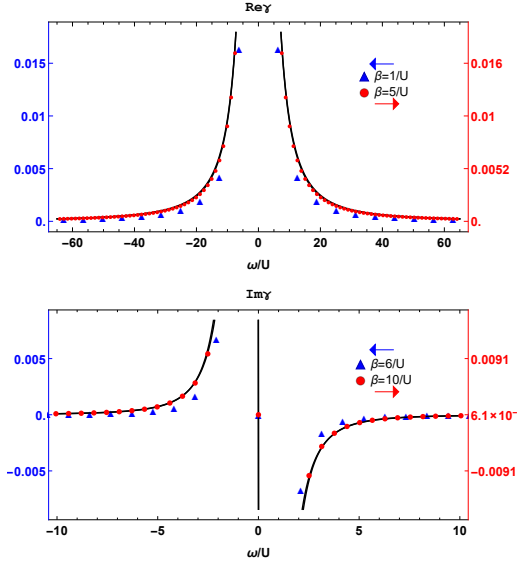


Figure 1. Real (top) and imaginary (bottom) parts of the phase correlator: numerical result (solid line) vs. two-term winding-number approximation (colored symbols at Matsubara frequencies) for $\mu/U = 0.4$. Each panel shows two temperatures: a lower one with good agreement (right vertical axis) and a higher one where deviations become noticeable (left vertical axis).

frequencies in Eq. (12) can be performed analytically. This, however, puts a practical limitation on including more winding numbers, as the process is significantly more complicated the higher is the order of the polynomials involved. As a result, a different approach to taking more terms in the winding number expansion would be desirable for a broader temperature range of the approximated correlator.

B. Expansion on an auxiliary variable

To obtain a broad temperature approximation for the correlator, we define the following function $S(x)$ of an auxiliary variable x :

$$S(x) = \sum_n \frac{e^{-(an^2 x + bn x + cn)}}{d + n^2 + \frac{b}{a} n} \quad (17)$$

with complex parameters a , b , c , and d (being functions of μ , β and ω_m). Taking the first deriva-

tive of $S(x)$, one arrives at a differential equation:

$$S'(x) = -a \sum_n e^{-(an^2 x + bn x + cn)} + adS(x), \quad (18)$$

which cannot be solved in closed form. However, we note that the phase correlator in Eq. (13) can be written in terms of $S(x)$ in the limit $x \rightarrow 1$ as:

$$\gamma(\omega_m) = \frac{A}{Z_0} \lim_{x \rightarrow 1} S(x) \quad (19)$$

by choosing:

$$\begin{aligned} a &= \beta/2 & b &= -\beta(v(\mu) + i\omega_m) \\ c &= 0 \text{ (bosons)} & d &= (v(\mu) + i\omega_m)^2 - 1/4, \end{aligned} \quad (20)$$

with $A = -e^{\beta v^2(\mu)}$ and noting the discrete nature of the Matsubara frequencies, for which $e^{\pm \beta i\omega_m} = 1$. Since only the point $x = 1$ is important in Eq. (18), its first term can be expanded in a power series around this point, giving rise to a polynomial, for which the differential equation can be analytically solved at any finite order of the expansion. At order N , the approximate solution to $S(x)$ is

$$\begin{aligned} S_N(x) &= e^{adx} \left(C_N - aZ' e^{-ad} \sum_{j=0}^N (-1)^j \right. \\ &\quad \times \left\langle (an^2 + bn)^j \right\rangle' \frac{1}{(ad)^{1+j}} \\ &\quad \times \left. \left\{ 1 - e^{-ad(x-1)} \sum_{k=0}^j \frac{1}{k!} [ad(x-1)]^k \right\} \right), \end{aligned} \quad (21)$$

where C_N depends on the boundary conditions and $\langle \cdot \rangle'$ and Z' are the expectation values and the partition function, respectively, for the distribution $e^{-(an^2 + bn + cn)}$, $n \in \mathbb{Z}$. This leads to the approximation for the correlator (at $x \rightarrow 1$):

$$\gamma(\omega_m) \approx \frac{A}{Z} C_N e^{ad}. \quad (22)$$

The constant C_N can be determined from the value of $S(0)$, which can be expressed in terms of hypergeometric functions. For the problem at hand $Z' = e^{-\beta v^2(\mu)} Z_0$, which leads to the final expression for the correlator at N -th order of ex-

pansion given by

$$\begin{aligned} \gamma(\omega) \approx \sum_{j=0}^N \left\langle \left(n^2 + \frac{b}{a} n \right)^j \right\rangle_{Z_0} \frac{1}{(-d)^{1+j}} \\ \times \left[1 - e^{\frac{\beta}{2} d} \sum_{k=0}^j \frac{1}{k!} \left(\frac{\beta}{2} \right)^k (-d)^k \right], \quad (23) \end{aligned}$$

which can be shown to converge to the correlator in Eq. (13).

The fact that the sum in Eq. (17) runs over all integers n means that any shift $n \rightarrow n + k$ (with $k \in \mathbb{Z}$) leaves the correlator unchanged. In other words, since shifting the summation index does not alter $\gamma(\omega_m)$, one may think there is a freedom in choosing the parameters a, b, c and d . However, to preserve the even symmetry of the real part and the odd symmetry of the imaginary part under $\omega_m \rightarrow -\omega_m$, these parameters must be fix exactly as above. Any other assignment, even if equivalent only up to an integer shift, would break those symmetries, forcing a “re-symmetrization” analogous to what was done for the winding-number expansion (there, by defining the symmetric $\tilde{v}(\mu)$ mapping).[–]

Figure 2 shows the real and imaginary parts of the expansion in Eq. (23) at order $N = 1$. The real part is accurately reproduced at all temperatures except at $\omega_m = 0$ point, at which it is only accurate for temperatures below $\beta \sim 30/U$. This zero-frequency point is important because strongly affects the phase boundary and particle density via the Lagrange multiplier. For this reason, we handle it more carefully below, with the corresponding results summarized in Fig. 3. –

The imaginary part remains accurate only for $\beta \gtrsim 2.5/U$; two temperatures are shown in Fig. 2 to illustrate where the approximation begins to deviate from the numerical result. However, since the imaginary part becomes small at high temperatures in both the numerical result and the approximation, the auxiliary-variable expansion remains practically useful over a broader temperature range than the winding-number expansion at the same order.

The slower convergence of the imaginary part is due to the expansion of the $e^{i\beta\omega_m n x}$ factor. This can be improved by rewriting it as $e^{i2\pi\{nmx\}}$ for each Matsubara frequency $\omega_m = 2\pi m/\beta$ and then performing the Taylor expansion. However, this leads to an increase of the complexity of the resulting expressions while not meaningfully improving the quality of the approximation.

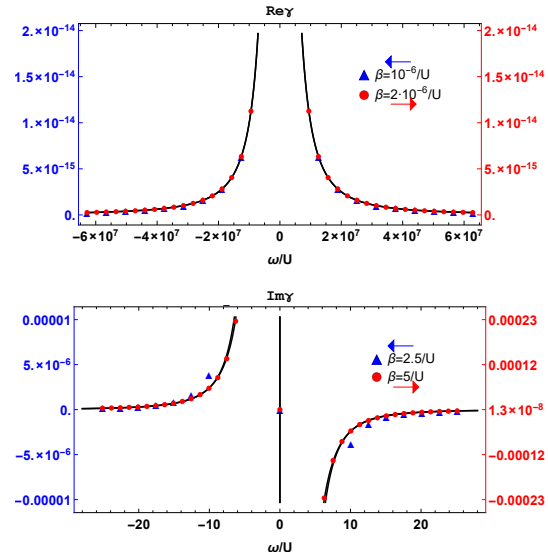


Figure 2. Real (top) and imaginary (bottom) parts of the phase correlator: numerical result (solid line) vs. two-term auxiliary-variable approximation (colored symbols at Matsubara frequencies) for $\mu/U = 0.4$. Each panel shows two temperatures. In the top panel, both temperatures display excellent agreement, indicating that the approximation remains accurate even at high temperature. In the bottom panel, the lower temperature still shows good agreement (right vertical axis), while the higher temperature illustrates the onset of deviation (left vertical axis).

Regarding the failure of this expansion to retrieve the correct value of the real part of the correlator at $\omega_m = 0$ at low orders of expansion, one could simply use the value from the numerical calculation of the correlator at this point. Nevertheless, it is possible to obtain a closed form expression in terms of special functions by rewriting the $\sum e^{-(an^2 x + bnx + cn)}$ term in Eq. (18) in terms of the Jacobi theta function $\vartheta_3(z, q)$:

$$\begin{aligned} \sum e^{-(an^2 x + bnx + cn)} = e^{\frac{(c + bx)^2}{4ax}} \sqrt{\frac{\pi}{ax}} \\ \times \vartheta_3 \left(\frac{\pi(c + bx)}{2ax}, e^{-\frac{\pi^2}{ax}} \right) \quad (24) \end{aligned}$$

and taking the series expansion only in ϑ_3 , lead-

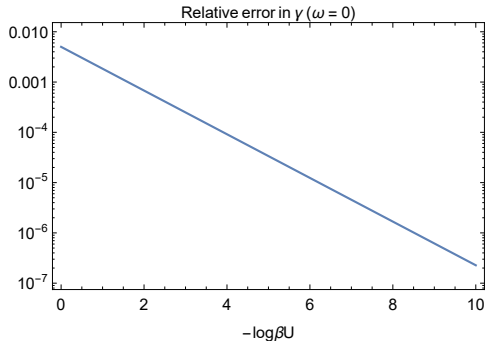


Figure 3. Decrease of the relative error in the estimation of $\gamma(\omega_m = 0)$ in Eq. (25) with the numerically evaluated value of Eq. (13) for summation over $n = -300, \dots, 300$ while the temperature is being increased.

ing to

$$\begin{aligned} \gamma(\omega_m) \approx & \frac{2\pi}{Z} e^{-\frac{\beta}{2}d} \left(\operatorname{Im} \left(\operatorname{erf} \left(i\sqrt{\frac{\beta}{8}} \right) \right) \right. \\ & - 2 \cos(2\pi(v(\mu) + i\omega_m)) \\ & \left. \times \operatorname{Im} \left(\operatorname{erf} \left(\pi\sqrt{\frac{2}{\beta}} - i\sqrt{\frac{\beta}{8}} \right) \right) \right), \quad (25) \end{aligned}$$

where $\operatorname{erf}(z) = \frac{2}{\sqrt{\pi}} \int_0^z e^{-t^2} dt$ is the complex error function. The expression in Eq. (25) not only works near $\omega_m = 0$ but also gets better the higher the temperature is, as shown in Figure 3.

In order to justify the success of this expansion in reproducing the correct values of the correlator at arbitrarily high temperatures, it is convenient to rewrite the phase correlator in Eq. (13) as

$$\begin{aligned} \gamma(\omega_m) = & \frac{\beta}{2} \int_{-1}^0 dt e^{-\beta t d(\omega_m)/2} \\ & \times \left\langle e^{-\beta t (n^2/2 - nv(\mu) - i\omega_m n)} \right\rangle_{Z_0}. \quad (26) \end{aligned}$$

Both schemes in effect only expand the expectation-value part inside the integral: winding numbers expand around $\beta \rightarrow \infty$ (low temperatures) and the auxiliary variable is equivalent to expansion around $\beta \rightarrow 0$ (high temperatures). Crucially, both leave the overall factor $e^{-\beta t d(\omega_m)/2}$ untouched, so even the high- T (auxiliary-variable) expansion continues to capture the dominant low-temperature behavior correctly.

IV. BOSE HUBBARD MODEL AT FINITE TEMPERATURES

Making use of the approximations for the phase correlator discussed in the previous section, it is possible to obtain analytical expressions for the critical line and the particle density at non-zero temperatures. The focus will be on temperatures corresponding to $\beta \gtrsim 5/U$, and hence, the appropriate and sufficient choice for the approximation of the phase correlator is a two-winding number expansion, which also facilitates analytical calculations. For instance, after performing the Matsubara summation in Eq. (12), the order parameter is given by

$$\begin{aligned} 1 - \psi^2 = & -\frac{e^{-\beta\tilde{v}^2(\mu)/2} + e^{-\beta(\tilde{v}(\mu)+1)^2/2}}{2Z_0} \\ & \times \int dx \rho(x) \sum_{j=1}^3 \coth \beta r_j(x)/2 \\ & \times \frac{\tilde{v}(\mu) + r_j(x) + \frac{1}{2} \frac{3e^{-\beta\tilde{v}^2(\mu)/2} - e^{-\beta(\tilde{v}(\mu)+1)^2/2}}{e^{-\beta\tilde{v}^2(\mu)/2} + e^{-\beta(\tilde{v}(\mu)+1)^2/2}}}{\prod_{i \neq j} (r_j(x) - r_i(x))}, \quad (27) \end{aligned}$$

where $z = r_j(x)$ are the zeros of the now rational function $D(z, x) = 1 + c(x)\gamma(z)$, which results from the denominator of the propagator in Eq. (9) with factored out $\gamma^{-1}(z)$, namely $\gamma^{-1}(z) [1 + (\lambda - |b_0|^2 x) \gamma(z)]$, which leads to $c(x) = \lambda - |b_0|^2 x$. In general, at the N -th order of the winding number expansion:

$$\begin{aligned} 1 - \psi^2 = & -\frac{\sum_{j=2-N}^{N-1} e^{-\beta(\tilde{v}(\mu)+j)/2}}{2Z_0} \\ & \times \int dx \rho(x) \coth \beta r_j(x)/2 \\ & \times \sum_{j=1}^{N+1} \frac{\prod_{i=1}^{N-1} (r_j(x) - q_i)}{\prod_{i \neq j} (r_j(x) - r_i(x))}, \quad (28) \end{aligned}$$

with $z = q_i$ being the zeros of the extension of the phase correlator to the whole complex plane, $\gamma(q_i) = 0$.

We can then easily obtain the phase diagram, i.e. the lines, where the order parameter ψ vanishes. Figure 4 shows the phase diagram in the $\mu - t$ parameter space at different temperatures. It shows how the low temperature lobe structure of the Mott insulator progressively fades away when increasing the temperature, as well as an increase on the hopping strength needed to reach

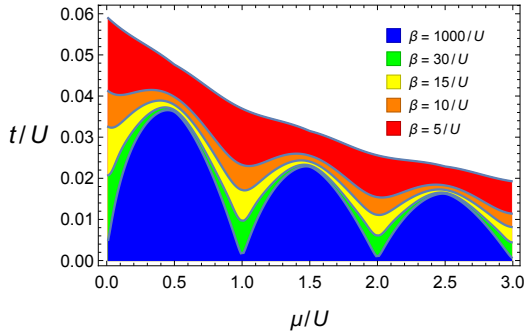


Figure 4. Phase diagram at different temperatures.

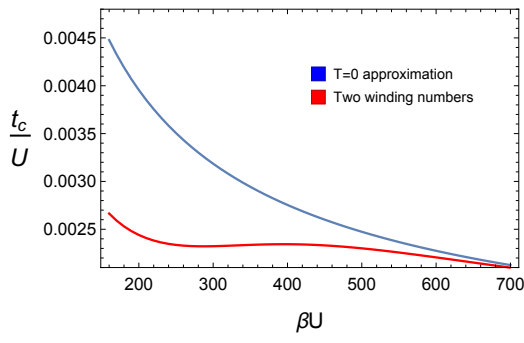


Figure 5. Comparison between the critical hopping parameter at $\mu/U = 1$ for the zero temperature approximation and the winding number expansion with two terms.

a long range phase coherent state in order to compensate for the increasing temperature fluctuations.

We can also use the above results to assess the region of validity of the original QRA approach with the zero-temperature correlator. In Figure 5 we have shown a comparison between the critical hopping parameter at $\mu/U = 1$ of the QRA with the zero-temperature correlator and the winding number expansion. Although, the deviation occurs even for very low temperatures, it becomes visibly significant for $k_B T/U \approx 0.002$ ($\beta U \approx 460$, where the deviation exceeds 10%). The zero temperature approximation leads not only quantitative differences with respect to the finite temperature corrections, but also qualitative, such as a sharpening of the phase diagram around integer values.

Next, we obtain an analytical expression for the particle density $n = df/d\mu$ (with $f = -(\beta N)^{-1} \ln Z$ being the free energy per particle) in terms of the order parameter, the zeros (r_j)

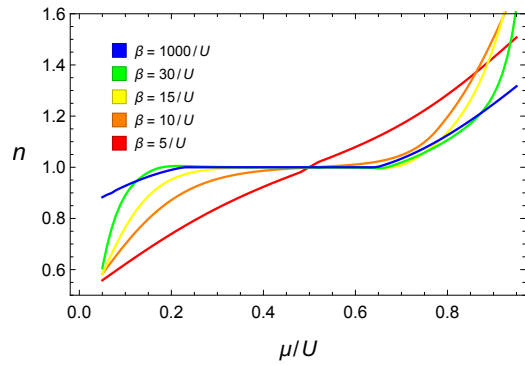


Figure 6. Particle density at different temperatures for hopping strength $t/U = 0.03$.

and the poles (p_j) of $D(z, x) = 1 + c(x)\gamma(z)$:

$$n = |\psi|^2 \partial_\mu \lambda + \bar{\mu} + \frac{1}{\beta} \partial_\mu \ln Z_0 + \frac{1}{\beta} \partial_\mu \int dx \rho(x) \ln \left(-\frac{\prod \sinh \beta r_j(x)/2}{\prod \sinh \beta p_j(x)/2} \right) + \frac{1}{2} \partial_\mu \int dx \rho(x) \sum (s(r_j) r_j - s(p_j) p_j), \quad (29)$$

where $s(z)$ is a sign function,

$$s(z) = \begin{cases} 1 & \text{Re}z \leq 0 \\ -1 & \text{Re}z > 0 \end{cases}. \quad (30)$$

Note that since the roots come in conjugate pairs and the poles are real, it is irrelevant in which of the two cases $\text{Re}z = 0$ is included.

Figure 6 shows the particle density at different temperatures in terms of the chemical potential for a fixed hopping strength $t/U = 0.03$. We can clearly observe the fixed integer density in the Mott insulator at low temperature, while the increase of temperature makes the density evolve towards a linear relation. The results corroborate theoretical predictions [16, 33] and experimental observations [4, 5]. The incompressible Mott-insulating phase begins to melt around $k_B T/U \approx 0.1$, where the density plateau in μ contracts; by $k_B T/U \approx 0.2$ the Mott lobes are washed out and $n(\mu)$ is almost linear.

The particle density can be also written in a more general way to accommodate approximations of the correlator $\gamma(\omega_m)$ in Eq. (13), which cannot be expressed as rational expressions (this applies also when the correlator is evaluated purely numerically). In such case, when $D(z, x)$

is no longer rational function:

$$\begin{aligned}
n = & |\psi|^2 \partial_\mu \lambda + \bar{\mu} + \frac{1}{\beta} \partial_\mu \ln Z_0 \\
& + \partial_\mu \int dx \rho(x) \frac{1}{\beta} \sum_\omega \ln(D(i\omega, x)) \\
& + \frac{1}{4\pi i} \partial_\mu \int dx \rho(x) \left(\oint_{\Gamma_-} dz \frac{z D'(z, x)}{D(z, x)} \right. \\
& \left. - \oint_{\Gamma_+} dz \frac{z D'(z, x)}{D(z, x)} \right) \quad (31)
\end{aligned}$$

with Γ_- (Γ_+) being a counterclockwise contour in the left (right) half-plane containing all roots and poles in that half, and $D'(z, x)$ denotes the derivative with respect to the complex variable z .

The function $D(z, x)$ has the same number of poles and zeros in each half-plane, so the branch cuts of $\ln D(z, x)$ can be chosen by forming pairs in between them, allowing the creation of contours on each half-plane that do not cross any branch cuts and still contain all zeros and poles of $D(z, x)$. Thus, the last term can be rewritten as an integral of $\ln D(z, x)$, which choosing large semicircles as contours, gives:

$$\begin{aligned}
n = & |\psi|^2 \partial_\mu \lambda + \bar{\mu} + \frac{1}{\beta} \partial_\mu \ln Z_0 \\
& + \partial_\mu \int dx \rho(x) \left(\frac{1}{\beta} \sum_m \ln(D(i\omega_m, x)) \right. \\
& \left. - \frac{1}{2\pi} \int_{-\infty}^{\infty} d\omega \ln(D(i\omega_m, x)) \right). \quad (32)
\end{aligned}$$

The last term is now seen as the difference between the finite temperature Matsubara sum of $D(z, x)$ and the sum at zero temperature. In cases where the Matsubara sum cannot be performed analytically and/or is computationally expensive (specially taking into account that it will have to be averaged with respect to the density of states), one can make use of the Euler-Maclaurin formula, which only requires information about the derivatives of $\ln D(z, x)$ at $z = 0$, and take advantage of the rapid decrease of $B_k/k!$, with

B_k the k -th Bernoulli number:

$$\begin{aligned}
n = & |\psi|^2 \partial_\mu \lambda + \bar{\mu} + \frac{1}{\beta} \partial_\mu \ln Z_0 \\
& + \frac{1}{2\beta} \partial_\mu \int dx \rho(x) D(0, x) \\
& - \frac{1}{\beta} \sum_{k=2}^{\infty} \frac{B_k}{k!} \partial_\mu \int dx \rho(x) D^{(k-1)}(0, x), \quad (33)
\end{aligned}$$

where $D^{(k)}(0, x)$ is the k -th derivative of $D(z, x)$ with respect to z evaluated at $z = 0$ and the sum can be truncated at finite order.

V. CONCLUSIONS

We have extended the quantum-rotor approach (QRA) to correctly include thermal fluctuations, providing a practical analytic tool for studying the Bose-Hubbard model at finite temperature. The zero-temperature phase correlator of Ref. [18] is now replaced by two complementary schemes: (i) a systematic expansion that keeps higher winding numbers, and (ii) an auxiliary-variable representation that rewrites functions of the form $f(\omega) = \sum_n f_n(\omega)$ via a Feynman-type integral identity. Both schemes yield closed-form expressions for the correlator as a function of Matsubara frequency, allowing seamless integration into the QRA framework. While the winding-number expansion already covers the temperature range relevant to optical-lattice experiments, the auxiliary-variable method is more general and should prove valuable in related problems that require even higher temperature.

With this extension we have computed the finite-temperature phase diagram of the Bose-Hubbard model together with the particle-density profile. The results corroborate theoretical predictions [16, 33] and experimental observations [4, 5], namely they correctly predict the melting of the incompressible Mott-insulating phase at temperatures around $k_B T/U \approx 0.1$, and loss of the Mott lobes by $k_B T/U \approx 0.2$. We have further shown that the original QRA already breaks down at $k_B T/U \approx 0.0022$, whereas the present formulation remains easily accurate for $k_B T \gtrsim U$ – well beyond the regime required for current experiments.

Beyond the observables presented here, the finite-T QRA retains the versatility of its $T = 0$ parent. It can therefore be applied directly to momentum-resolved spectral functions, structure

factors, and transport kernels also in synthetic gauge fields at experimentally relevant temperatures. The formalism also prepares the ground for incorporating amplitude (Higgs) fluctuations, which are essential above $k_B T/U \approx 0.2$.

In summary, this work closes the temperature gap that has separated analytic QRA predictions from ultracold-atom data, providing a transparent and computationally efficient framework for exploring strongly correlated lattice bosons in the finite-entropy regimes accessible to experiment.

ACKNOWLEDGEMENTS

Acknowledgments. This research was funded in whole or in part by National Science Centre, Poland within PRELUDIUM BIS-2 UMO-2020/39/O/ST3/01148 project.

Data availability. The data that support the findings of this paper are openly available [34].

- [1] M. P. A. Fisher, P. B. Weichman, G. Grinstein, and D. S. Fisher, Boson localization and the superfluid-insulator transition, *Phys. Rev. B* **40**, 546 (1989).
- [2] D. Jaksch, C. Bruder, J. I. Cirac, C. W. Gardiner, and P. Zoller, Cold Bosonic Atoms in Optical Lattices, *Phys. Rev. Lett.* **81**, 3108 (1998).
- [3] M. Greiner, O. Mandel, T. Esslinger, T. W. Hänsch, and I. Bloch, Quantum phase transition from a superfluid to a Mott insulator in a gas of ultracold atoms, *Nature* **415**, 39 (2002).
- [4] W. S. Bakr, A. Peng, M. E. Tai, R. Ma, J. Simon, J. I. Gillen, S. Fölling, L. Pollet, and M. Greiner, Probing the Superfluid-to-Mott Insulator Transition at the Single-Atom Level, *Science* **329**, 547 (2010).
- [5] J. F. Sherson, C. Weitenberg, M. Endres, M. Cheneau, I. Bloch, and S. Kuhr, Single-atom-resolved fluorescence imaging of an atomic Mott insulator, *Nature* **467**, 68 (2010).
- [6] I. Bloch, J. Dalibard, and W. Zwerger, Many-Body Physics with Ultracold Gases, *Rev. Mod. Phys.* **80**, 885 (2008), 0704.3011.
- [7] D. C. McKay and B. DeMarco, Cooling in strongly correlated optical lattices: prospects and challenges, *Rep. Prog. Phys.* **74**, 054401 (2011).
- [8] M. Miranda, R. Inoue, N. Tambo, and M. Kozuma, Site-resolved imaging of a bosonic Mott insulator using ytterbium atoms, *Phys. Rev. A* **96**, 043626 (2017).
- [9] K. Kwon, K. Kim, J. Hur, S. Huh, and J.-y. Choi, Site-resolved imaging of a bosonic Mott insulator of ^7Li atoms, *Phys. Rev. A* **105**, 033323 (2022).
- [10] B. Yang, H. Sun, C.-J. Huang, H.-Y. Wang, Y. Deng, H.-N. Dai, Z.-S. Yuan, and J.-W. Pan, Cooling and entangling ultracold atoms in optical lattices, *Science* **369**, 550 (2020).
- [11] D. B. M. Dickerscheid, D. van Oosten, P. J. H. Denteneer, and H. T. C. Stoof, Ultracold atoms in optical lattices, *Phys. Rev. A* **68**, 043623 (2003).
- [12] X. Lu, J. Li, and Y. Yu, Slave-particle approach to the finite-temperature properties of ultracold Bose gases in optical lattices, *Phys. Rev. A* **73**, 043607 (2006).
- [13] L. I. Plimak, M. K. Olsen, and M. Fleischhauer, Occupation number and fluctuations in the finite-temperature Bose-Hubbard model, *Phys. Rev. A* **70**, 013611 (2004).
- [14] B. DeMarco, C. Lannert, S. Vishveshwara, and T.-C. Wei, Structure and stability of Mott-insulator shells of bosons trapped in an optical lattice, *Phys. Rev. A* **71**, 063601 (2005).
- [15] B. Capogrosso-Sansone, i. m. c. G. m. c. Söyler, N. Prokof'ev, and B. Svistunov, Monte Carlo study of the two-dimensional Bose-Hubbard model, *Phys. Rev. A* **77**, 015602 (2008).
- [16] K. W. Mahmud, E. N. Duchon, Y. Kato, N. Kawashima, R. T. Scalettar, and N. Trivedi, Finite-temperature study of bosons in a two-dimensional optical lattice, *Phys. Rev. B* **84**, 054302 (2011).
- [17] B. Capogrosso-Sansone, N. V. Prokof'ev, and B. V. Svistunov, Phase diagram and thermodynamics of the three-dimensional Bose-Hubbard model, *Phys. Rev. B* **75**, 134302 (2007).
- [18] T. P. Polak and T. K. Kopec, Quantum rotor description of the Mott-insulator transition in the Bose-Hubbard model, *Phys. Rev. B* **76**, 094503 (2007).
- [19] T. A. Zaleski and T. K. Kopec, Atom-atom correlations in time-of-flight imaging of ultracold bosons in optical lattices, *Phys. Rev. A* **84**, 053613 (2011).
- [20] T. A. Zaleski and T. P. Polak, Synthetic magnetic field effects on neutral bosonic condensates in quasi-three-dimensional anisotropic layered structures, *Phys. Rev. A* **83**, 023607 (2011).
- [21] T. P. Polak and T. A. Zaleski, Time-of-flight patterns of ultracold bosons in optical lattices in various Abelian artificial magnetic field gauges, *Phys. Rev. A* **87**, 033614 (2013).
- [22] T. A. Zaleski, Momentum-resolved spectral function of ultracold bosons in two-dimensional op-

tical lattices, *Phys. Rev. A* **85**, 043611 (2012).

[23] T. A. Zaleski, Optical weight transfer in excitation spectra of ultra-cold bosons in two- and three-dimensional optical lattices, *J. Phys. B: At. Mol. Opt. Phys.* **45**, 145303 (2012).

[24] T. Zaleski and T. Kopeć, Coherence and spectral weight transfer in the dynamic structure factor of cold lattice bosons, *Physica B* **504**, 74 (2017).

[25] B. Grygiel and T. A. Zaleski, Momentum-resolved conductivity of strongly interacting bosons in an optical lattice, *Phys. Rev. B* **104**, 104511 (2021).

[26] T. Zaleski and T. Kopeć, Temperature-dependent excitation spectra of ultra-cold bosons in optical lattices, *Physica B* **433**, 37 (2014).

[27] T. Zaleski and T. Kopeć, Finite temperature superfluid transition of strongly correlated lattice bosons in various geometries, *Physica B* **456**, 244 (2015).

[28] T. H. Berlin and M. Kac, The Spherical Model of a Ferromagnet, *Phys. Rev.* **86**, 821 (1952).

[29] G. S. Joyce, Spherical Model with Long-Range Ferromagnetic Interactions, *Phys. Rev.* **146**, 349 (1966).

[30] T. P. Polak and T. K. Kopec, Frustration effects in rapidly rotating square and triangular optical lattices, *Phys. Rev. A* **79**, 063629 (2009).

[31] T. A. Zaleski and T. K. Kopeć, Effect of next-nearest-neighbour hopping on Bose-Einstein condensation in optical lattices, *J. Phys. B: At. Mol. Opt. Phys.* **43**, 085303 (2010).

[32] T. A. Zaleski and T. K. Kopeć, Superfluid-to-Mott transition in optical lattices with restricted geometry, *J. Phys. A: Math. Theor.* **43**, 425303 (2010).

[33] F. Gerbier, Boson Mott Insulators at Finite Temperatures, *Phys. Rev. Lett.* **99**, 120405 (2007).

[34] T. A. Zaleski and M. Rodríguez-Martín, Data for "Finite-Temperature Quantum-Rotor Approach for Ultracold Bosons in Optical Lattices" (2025).